Latin American Journal of Solids and Structures
www.lajss.org

Sensitivity Analysis of the Effectiveness of Tuned Mass Dampers to Reduce the Wind-Induced Torsional Responses

Abstract

Use of Tuned Mass Dampers (TMDs) to reduce the wind-induced torsional response of structures has been investigated in the literature by assuming that the wind excitations can be approximated by harmonic forces or white noise random processes; however, such an assumption is not realistic. Further, wind load effects are correlated. This study is focused on the effectiveness of different linear/nonlinear TMDs configurations to reduce the wind induced response. For the analyses, the structure is modeled as a multi-degree of freedom system under correlated wind load effects. The results show that the selection of optimum dampers is affected by the consideration of the correlated wind load effects.

Keywords

Tuned mass dampers, Torsional response, Nonlinear TMDs, Simulation of wind forces, Structural control.

A. Pozos-Estrada [a]
H.P. Hong [b]

[a] Instituto de Ingeniería, Universidad Nacional Autónoma de México, Ciudad de México, México, C.P. 04510, APozosE@iingen.unam.mx
[b] Department of Civil and Environmental Engineering, The University of Western Ontario, Canada N6A 5B9, hhong@uwo.ca

http://dx.doi.org/10.1590/1679-78251856

Received 19.01.2015
Accepted 04.08.2015
Available online 25.08.2015

1 INTRODUCTION

The use of passive energy dissipation devices to reduce peak responses of structures has been investigated, and their performance for wind and earthquake induced responses are considered to be satisfactory and promising (Housner et al., 1997). One of the passive energy dissipation systems is the tuned mass damper (TMD) which is used to control the response of tall buildings or slender structures subjected to wind or earthquake excitations. A TMD consists of a mass which is connected to the structure through a spring and a dashpot (i.e., damper) in parallel. The TMD is activated by the wind or earthquake induced structural motion; the kinetic energy is transmitted from the structure to the TMD and is dissipated by the damper. The main objective of using the TMD is to reduce the structural responses to satisfy criteria for serviceability or ultimate limit states. A highest reduction of the structural peak response could be achieved by tuning or selecting the parameters of the TMD such as the frequency ratio and damping ratio. The selection of the optimum parameters

of the TMD has been carried out as earlier as the 1950s by Den Hartog (1956) considering undamped systems. Warburton (1982) developed equations for evaluating the optimum parameters of the TMD considering the main structure as an undamped SDOF system for various combinations of response and excitation. Warburton and Ayorinde (1980) studied the effect of the damping of the structure on the optimum parameters of the TMD and showed that it is possible to represent a complex mechanical system by means of an equivalent SDOF system if its natural frequencies are well separated. In all the above-mentioned studies, the harmonic or white noise excitations are used to define the selection of the optimum parameters of the TMD, even though they may not adequately represent the characteristics of the strong wind or large earthquake induced excitations.

More recently, the use of multiple TMDs to reduce the peak responses of structures, that are sensitive to torsional effects, has been reported by Jangid and Data (1997), Pansare and Jangid (2003), Li and Qu (2006), Bakre and Jangid (2007) , and Wang et al. (2009). The excitations considered in these studies do not differ from those mentioned previously. For instance, Jangid and Data (1997), Bakre and Jangid (2007), and Wang et al. (2009) used an exciting force represented by band limited white-noise; Pansare and Jangid (2003) and Li and Qu (2006) analysed structures subjected to external harmonic excitations. The damping mechanism of the TMDs (i.e. dashpot) was modeled as linear or viscous in most of these studies. The assumption of viscous damping simplifies the analysis, even though it may not be realistic due to friction or the properties of the fluid used in the dashpot, which are temperature dependent. A state space linear mathematical model has been proposed by Mattei and Ricciardelli (2002), where a detail treatment of the wind loading is carried out; unfortunately, no guidelines on the applicability to practical problems of the proposed model is given.

Attention has also been paid to the use of nonlinear TMDs, such as the use of power law and dry-friction damping mechanisms which occur commonly in practice, to suppress the structural response. For example, the use of the power law damping mechanism has been studied by Terenzi (1999), Vickery et al. (2001) and Rüdinger (2007a, 2007b); whereas Ricciardelli and Vickery (1999) explored the use of tuned vibrations absorbers with dry friction damping and linear stiffness.

The main objective of the present study is to assess the effectiveness of different TMDs configurations with linear and nonlinear damping mechanisms (i.e. viscous damping and power law damping mechanism) with different location on a structure to reduce the wind induced torsional responses. The assessment is focused on parametric investigations by considering possible combinations of parameters and locations of the TMDs. Rather than using the harmonic or white noise excitations to represent the wind loading, a more realistic characterization of the wind excitations that is based on the power spectral density (PSD) function of the fluctuating wind forces is considered. Time history analyses were carried out to evaluate the structural peak response under the simulated wind loading that is characterized by the adopted PSD function.

2 MODEL, PEAK RESPONSES AND OPTIMUM TMD SYSTEM

2.1 TMD-structure system and equation of motion

Consider a structure that is modeled as a two-degree-of-freedom system (lateral displacement Y and rotational displacement θ) with mass M_s, and mass moment of inertia I_s. The structure is shown in

Figure 1a. The lateral and torsional stiffness of the structure are denoted by K_s and K_θ, respectively; the damping coefficients of the structure for the lateral and rotational directions are represented by C_s and C_θ, respectively.

The equation of motion of the structure under wind loading can be expressed as

$$\begin{bmatrix} M_S & 0 \\ 0 & I_S \end{bmatrix} \begin{Bmatrix} \ddot{Y} \\ \ddot{\theta} \end{Bmatrix} + \begin{bmatrix} C_S & 0 \\ 0 & C_\theta \end{bmatrix} \begin{Bmatrix} \dot{Y} \\ \dot{\theta} \end{Bmatrix} + \begin{bmatrix} K_S & 0 \\ 0 & K_\theta \end{bmatrix} \begin{Bmatrix} Y \\ \theta \end{Bmatrix} = \begin{Bmatrix} F_Y(t) \\ M(t) \end{Bmatrix} \tag{1}$$

where F_Y(t) and M(t) represent, respectively, the total horizontal force and the torsional moment due to fluctuating wind loading that will be discussed in the next section; a dot on a symbol denotes its temporal derivative (i.e., velocity); and a double-dot on a symbol denotes second temporal derivative (i.e., acceleration).

Now consider that the structure is fitted with three TMDs as illustrated in Figure 1b. The use of three TMDs, especially the two that are away from the center of mass, is aimed at reducing peak torsional structural responses, while all three TMDs can be used to reduce the lateral response of the structure. The TMDs are connected to the structure by linear/nonlinear dashpots and linear elastic springs; the nonlinear damping form considered in this study is power law. The TMDs are characterized by the mass ratio μ representing the ratio of the mass of the TMDs to the mass of the main structure, and by the frequency ratio r_f defined as the ratio of the frequency of the TMD to the frequency of the vibration mode of the main structure whose response is to be reduced. The stiffness of the TMD can be readily calculated if the above mentioned ratios and the properties of the main structure are known.

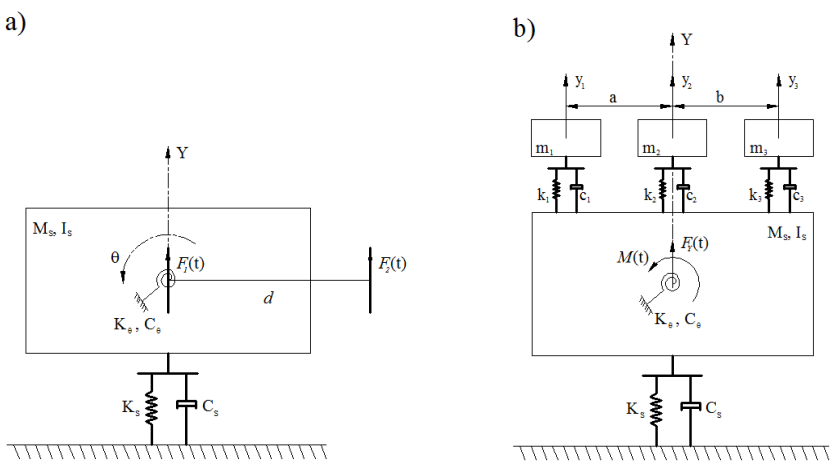

Figure 1: Structure without and with TMDs: a) Structure without TMDs, b) Structure with TMDs.

The equation of motion of the TMD-structure system shown in Figure 1b can be expressed in matrix form as

$$[M]\{\ddot{X}(t)\} + \{F_{DT}(\dot{X}(t))\} + [K]\{X(t)\} = \{F(t)\} \tag{2a}$$

where

$$[M]=\begin{bmatrix} M_S & 0 & 0 & 0 & 0 \\ 0 & I_S & 0 & 0 & 0 \\ 0 & 0 & m_1 & 0 & 0 \\ 0 & 0 & 0 & m_2 & 0 \\ 0 & 0 & 0 & 0 & m_3 \end{bmatrix} \tag{2b}$$

$$[K]=\begin{bmatrix} K_S+k_1+k_2+k_3 & bk_3-ak_1 & -k_1 & -k_2 & -k_3 \\ & K_\theta+a^2k_1+b^2k_3 & ak_1 & 0 & -bk_3 \\ & & k_1 & 0 & 0 \\ & symm & & k_2 & 0 \\ & & & 0 & k_3 \end{bmatrix} \tag{2c}$$

$$\{X(t)\}=[Y \quad \theta \quad y_1 \quad y_2 \quad y_3]^T \tag{2d}$$

$$\{F(t)\}=[F_Y(t) \quad M(t) \quad 0 \quad 0 \quad 0]^T \tag{2e}$$

$$\{F_{DT}(\dot{X}(t))\}=\begin{Bmatrix} C_S\dot{Y}+F_{D1}(\dot{Y}-a\dot{\theta}-\dot{y}_1)+F_{D2}(\dot{Y}-\dot{y}_2)+F_{D3}(\dot{Y}+b\dot{\theta}-\dot{y}_3) \\ C_\theta\dot{\theta}-aF_{D1}(\dot{Y}-a\dot{\theta}-\dot{y}_1)+bF_{D3}(\dot{Y}+b\dot{\theta}-\dot{y}_3) \\ -F_{D1}(\dot{Y}-a\dot{\theta}-\dot{y}_1) \\ -F_{D2}(\dot{Y}-\dot{y}_2) \\ -F_{D3}(\dot{Y}+b\dot{\theta}-\dot{y}_3) \end{Bmatrix} \tag{2f}$$

in which m_i, k_i and y_i , $i = 1,2,3$, are the mass, stiffness and displacement of the i-th mass damper (see Figure 1b); and $F_{Di}(v)$, $i = 1,2,3$, represents damping force of the i-th mass damper that depend on the velocity, v,.

As mentioned above, the two functional forms of damping force considered in this study are the viscous case and the power law damping mechanism. For simplicity and practical considerations, it is considered that the same type of damper is to be installed in a structure. This implies that the functional form for $F_{Di}(v)$, $i = 1,2,3$, are the same as $F_D(v)$.

$$F_D(v)=C_L v \tag{3}$$

if the viscous damping mechanism is considered, and

$$F_D(v) = C_{PL} sign(v)|v|^{\beta} \tag{4}$$

if the power law damping mechanism is considered. In Eqs. (3) and (4), C_L is a viscous damping coefficient; C_{PL} is a power law viscous damping coefficient; $|\bullet|$ denotes the absolute value of its argument; β is a model parameter within the range 0.5 to 2 (Soong and Costantinou, 1994), a value of 2 is selected for the parametric analysis.

It is noteworthy that if one or two rather than three TMDs are considered, Eq. (2) can be reduced accordingly and used to describe the motion of the system.

2.2 Wind Loading and Analysis Procedure

Wind speed is often represented by a mean wind component and a fluctuating wind component. The fluctuating component varies in time, is stochastic and characterized by its PSD function. The well-known PSD functions for the turbulent wind speed include the ones given by Kolgomorov, von Karman, Davenport, Harris, Kaimal (Simiu and Scanlan, 1996). The forces or pressures induced by wind can be viewed as the sum of the mean wind force and the fluctuating wind force which is directly proportional to the fluctuating wind speed, if the quadratic term of the fluctuating wind speed is ignored. In this study, it is considered that the PSD function of the normalized fluctuating wind force, $S(f)$, can be expressed as

$$S(f) = \begin{cases} Af^{-(1+\alpha)} & f_L \le f \le f_U \\ 0 & \text{otherwise} \end{cases} \tag{5}$$

where f_L and f_U are upper and lower bounds of f, α is an exponent that depends on the direction of the wind velocity, f is frequency in Hz, and A is a normalization constant such that the integration of the PSD function equals one. The adoption of this PSD function is justified since boundary layer wind tunnel test results (Pozos-Estrada et al., 2011) indicate that such a PSD function provides sufficient accurate characterization of the fluctuating wind force in the inertial subrange, which is of interest in the present study. It is noted that the value of f that most of the structures are sensitive to, especially tall buildings, falls within 0.05 to 0.5 (Hz).

Since structural geometric shapes vary and wind pressure acting on the structures are not necessarily symmetric, the spatially distributed wind pressure could induce both along wind vibration and torsional responses around the vertical axis. To simplify the parametric study, it is considered that the overall wind force acting on the structural model considered can be modeled as two uncorrelated horizontal along wind loads. These loads are proportional to $F_1(t)$ and $F_2(t)$, where their PSD functions are given by Eq. (5), and are acting at different points as shown in Figure 1a. In such a case, the total horizontal force $F_Y(t)$ and the torsional moment M(t) are given by

$$F_Y(t) = c\sqrt{1-\rho_{F_YM}{}^2}\,F_1(t) + \rho_{F_YM} cF_2(t) \tag{6a}$$

and

$$M(t) = R \times \left(\rho_{F_Y M} c F_2(t)\right) \tag{6b}$$

where c, R and $\rho_{F_Y M}$ are model parameters. R is the measure of the distance from the torsional center to the line of the eccentric force $\rho_{F_Y M} c F_2(t)$. It can be shown that $\rho_{F_Y M}$ represents the correlation coefficient between $F_Y(t)$ and $M(t)$, and that the ratio of the standard deviation of the $M(t)$, σ_M, to that of $F_Y(t)$, σ_F, for the wind loads defined in Eq. (6) is equal to $\rho_{F_Y M} R$. The latter indicates that the standard-deviation-based load eccentricity e_σ (i.e., σ_M/σ_F), equals $\rho_{F_Y M} R$. Use of Eq. (6) to model the wind loads is advantageous since it can be employed to match prescribed values of σ_F and e_σ by simply setting c equal to σ_F and R equal to $e_\sigma / \rho_{F_Y M}$. Note that in all cases, $M(t)$ can be expressed as $e_\sigma \sigma_F \times F_2(t)$ or $\sigma_M \times F_2(t)$.

Given the PSD function of the wind force, its time history can be simulated using, for example, the spectral representation method (Shinozuka, 1972), although more sophisticated algorithms can also be used (Di Paola, 1998). The method consists of using sum of a series of sine functions with random phase angles. More specifically, if a stationary stochastic process $Z(t)$ is characterized by its (one sided) PSD function $S_{ZZ}(f)$, a sample of the stochastic process, $z(t)$, can be expressed as

$$z(t) = \sqrt{2} \sum_{i=1}^{N} \sqrt{S_{ZZ}(f_i)\Delta f} \sin\left(2\pi f_i t + \phi_i\right) \tag{7}$$

where $f_i = i \times \Delta f$, $i = 1, 2, ..., N$, $\Delta f = 1/(N\Delta t)$, Δt is the time increment and φ_i is a uniformly distributed random variable within 0 to 2π. Therefore, by using this simulation approach, samples of $F_1(t)$ and $F_2(t)$ can be simulated if the parameters of the PSD function shown in Eq. (5), α, f_L and f_U are given. The simulated time series are then used in Eq. (6) to evaluate $F_Y(t)$ and $M(t)$ for given values of $\rho_{F_Y M}$, σ_F, and e_σ. The samples of $F_Y(t)$ and $M(t)$ can then be used in Eqs. (1) and (2) to calculate the response time history of the structure with and without the TMD system using the Newmark's method, and to assess the benefit of using the TMD system.

However, before providing the detailed analysis procedure to investigate the effectiveness of the TMD system, it is noteworthy that most of the existing studies mentioned in the introduction section considered that the use of the TMD systems is aimed at controlling the wind induced peak translational structural response, Y_p. It is known that excessive responses such as the peak rotational velocity, $\dot{\theta}_p$, and the translational acceleration at a point within the structural footprint, $\ddot{Y}_{pr}$, could also affect significantly the building occupants' comfort (Chen and Robertson, 1972; Irwin, 1978; Melbourne and Palmer, 1992; Isyumov, 1993; Isyumov, 1995; Pozos-Estrada et al., 2010). Therefore, one could also be interested in using the TMD systems to reduce these peak responses. Given the time history of the responses of duration T_d, a sample of the mentioned peak responses can be obtained from

$$Y_p = \max_{t \in [0, T_d]} \left| Y(t) \right| \tag{8a}$$

$$\dot{\theta}_p = \max_{t\in[0,T_d]} |\dot{\theta}(t)| \tag{8b}$$

$$\ddot{Y}_{pr} = \max_{t\in[0,T_d]} |\ddot{Y}(t) \pm \ddot{\theta}(t) r| \tag{8c}$$

where $Y(t)$ is the translational displacement; $\dot{\theta}(t)$ is the rotational velocity; $\ddot{Y}(t)$ and $\ddot{\theta}(t)$ are the lateral and rotational accelerations, respectively; and r is the distance from the point of interest within the structural footprint to the center of rotation of the main structure.

The effectiveness of the TMD system to reduce the peak responses can be measured using the ratios of the peak responses of the structure without and with a TMD system. These ratios are defined as

$$R_Y = Y_{pT} / Y_{pO} \tag{9a}$$

$$R_{\dot{\theta}} = \dot{\theta}_{pT} / \dot{\theta}_{pO} \tag{9b}$$

and

$$R_{\ddot{Y}} = \ddot{Y}_{prT} / \ddot{Y}_{prO} \tag{9c}$$

where the symbols Y_p, $\dot{\theta}_p$ and $\ddot{Y}_{pr}$ with an additional subscript O denote the (maximum) peak responses of the structure without a TMD system shown in Figure 1a, while those with an additional subscript T denote the (maximum) peak response of the structure with a TMD system shown in Figure 1b.

For a given structure and parameters defining the wind loading (i.e., parameters for Eqs. (6) and (7)), based on the above, the analysis procedure to assess the effectiveness of the TMD in suppressing the peak responses can be summarized as follows:

1) Sample a wind load time history by using the wind load model defined in Eq. (6) for a duration greater than Td, such that the useful time of the time history of the responses is equal to Td;
2) Evaluate the time history of the responses of the structure without and with a TMD system by solving, respectively, Eq. (1) and Eq. (2) using Newmark's method;
3) Evaluate the peak responses Y_{pO}, $\dot{\theta}_{pO}$ and $\ddot{Y}_{prO}$ of the structure without a TMD system and Y_{pT}, $\dot{\theta}_{pT}$ and $\ddot{Y}_{prT}$ of the structure with a TMD system. Evaluate R_Y, $R_{\dot{\theta}}$ and $R_{\ddot{Y}}$, defined in Eq. (9), employing the obtained peak responses;
4) Repeat Steps 1) to 3) n times to generate samples of R_Y, $R_{\dot{\theta}}$ and $R_{\ddot{Y}}$ to evaluate their mean values denoted by m_{RY}, $m_{R\dot{\theta}}$ and $m_{R\ddot{Y}}$.

The above procedure can also be used to calculate samples and statistics of the responses of the structure without or with TMD systems alone by simply solving Eq. (1) or Eq. (2) only in Step 2), and ignoring the evaluation of the ratios in Step 4).

2.3 Identification of optimum TMD system

For a given structure, the optimum TMD system is often defined as the one that minimizes the expected response ratio such as m_{RY}. In practice, the design of a TMD starts by setting the value of the mass ratio μ, which was defined previously. The value of μ is usually set within 1% to 10%

(Warburtun and Ayorinde, 1980). One of the considerations for selecting this parameter is the available space to place the TMD. Although the use of an increased mass ratio value helps to further reduce the response, it may not be feasible or economic since other structural elements may need to be strengthened due to the additional weight of the TMD. Once the value of the mass ratio has been selected, other parameters such as frequency ratio r_f and damping coefficients of the TMDs need to be selected for the TMDs. Several recommendations have been given to determine the optimum parameters of the TMD as a function of the mass ratio (Den Hartog, 1956; Tsai and Lin, 1983; Fujino and Abe, 1993; Vickery et al., 2001). These recommendations were developed based on harmonic excitations and white noise excitations for specific target translational responses only.

In this section, steps for identifying the optimum TMD system for specified mass ratios considering both translational and rotational responses are outlined. The identification of the optimum TMD system only needs to consider a combination of suitable ranges of the damping coefficient C (i.e., C_L or C_{PL}) of the TMD and r_f values. In order to identify the parameters leading to the optimum TMD system, numerical search algorithms can be used (Vanderplaats, 1984; Haupt and Haupt, 2004). The use of numerical algorithms for the identification is justified since no closed form solution is available for the considered types of TMD system under stochastic wind loads. Since only two parameters (C and r_f) need to be identified, a simple grid search procedure can be used. For a given mass ratio and a structural system approximated by the model shown in Figure 1b, this basically involves:

1) For a selected set of values of r_f and C, carry out dynamic analysis to evaluate m_{RY}, $m_{R\dot{\theta}}$ and $m_{R\ddot{Y}}$ as outlined previously;
2) Repeat Step 1) for a suitable range of r_f and C values, and identify the combination of r_f and C, denoted by (r_{fopt}, C_{opt}), that leads to the lowest m_{RY}, $m_{R\dot{\theta}}$ and/or $m_{R\ddot{Y}}$.

   The identified (r_{fopt}, C_{opt}) provides the optimum design for the TMD system.

3 PARAMETRIC STUDIES

3.1 Structural Characteristics and Peak Responses

For the analysis, an actual structure is approximated by a two-degree-of-freedom (2DOF) system whose characteristics are defined by the generalized properties of the actual structure. For the numerical example, the mass, M_s, and mass moment of inertia, I_s, of the generalized system, representing a 60 story tower, are considered to be equal to 2,519,208 kg and 2,472,771 kg-m2, respectively; the natural frequencies of the structure, defined as ω_Y and ω_θ, are equal to 0.753 and 0.959 rad/s. The damping ratios ζ_Y and ζ_θ for the sway and torsional mode are set equal to 1%. The stiffness and damping coefficient of the generalized system can be calculated from $K_s = M_s\omega_Y^2$, $C_s = 2\zeta_s\omega_Y M_s$, $K_\theta = I_s\omega_\theta^2$, $C_\theta = 2\zeta_s\omega_\theta I_s$.

By considering that the structure is subjected to the wind loads defined in Eqs. (5) to (7) with $\alpha = 1.5$, $\sigma_F = 27340$, $e_\sigma = 0.033$ and $\rho_{F_Y M} = 0$, the calculated mean of Y_{pO}, $\dot{\theta}_{pO}$ and $\ddot{Y}_{prO}$, by using the procedure outlined in the previous sections, are shown in Table 1. Note that σ_F and e_σ are cho-

sen such that the mean of Y_{pO}, $\dot{\theta}_{pO}$ and $\ddot{Y}_{prO}$ with a simulation cycle of 30 are equal to 0.292 m, 4.83x10-3 rad/s (4.8 milli-rad/s) and 0.267 m/s2 (27.2 milli-g), respectively, for T_d equal to 10 min. The considered values of $\dot{\theta}_{pO}$ and $\ddot{Y}_{prO}$ are associated with the response levels that could affect the comfort, health and/or disrupt the daily activities of the building occupants (Mendis et al., 2007; Isyumov, 1995), while the value of Y_{pO} is selected considering a drift ratio of about 1/667.

For the analysis the simulation cycle, n, is considered equal to 30, and T_d is considered to be equal to 10 minutes. To see whether this selected simulation cycle $n = 30$ is adequate to evaluate the peak mean responses, the analysis is repeated with $n = 60$, and the obtained mean of Y_{pO}, $\dot{\theta}_{pO}$ and $\ddot{Y}_{prO}$ are 0.289 m, 4.83 rad/s and 0.27 m/s^2, respectively. Comparison of these results to the previous ones suggests that the use of n =30 for evaluating the mean value is adequate. Therefore, unless otherwise indicated, n equal to 30 is adopted for the remaining numerical analyses.

$\rho_{F_Y M}$	Mean		
	Y_{pO} (m)	$\dot{\theta}_{pO}$ (rad/s)	$\ddot{Y}_{prO}$ (m/s^2)
0	0.292	4.82E-03	0.267
0.25	0.291	5.09E-03	0.276
0.5	0.304	4.94E-03	0.282
0.75	0.291	4.87E-03	0.263
1	0.295	4.82E-03	0.268

Table 1: Statistics of the peak responses of the main structure without TMDs.

To assess the impact of the correlation between the along wind load and the torsional moment on the responses, $\rho_{F_Y M}$ is varied from 0 to 1.0 with an increment of 0.25 while α, σ_F, and e_σ are maintained to be the same. The obtained results by repeating the above analysis are also listed in Table 1. The results show that the mean values of the responses of the structure without dampers are sufficiently uniform. This is due to that the values σ_F and e_σ (see Eq. (6)) are not affected by the selected $\rho_{F_Y M}$ value.

3.2 Responses with TMDs

To investigate the effectiveness of using the TMDs to suppress the peak responses of the considered structure, three basic TMD-structure systems are studied in the following.

In the first system, the structure is fitted with three identical TMDs (see Figure 1b) (i.e., the dampers have the same mass, stiffness and damping coefficient). The use of identical dampers placed at different locations has been used by Pansare and Jangid (2002) to mitigate the response of structures under sinusoidal force. This is consistent with the decisions often made in practice in reducing cost of manufacturing dampers. Use of this TMD-structure system is aimed at reducing both the lateral and torsional responses. The second system considers two dampers, each located at each side of the center of rotation of the main structure. The properties of these two dampers are

again considered to be the same; use of this system is focused mainly on the mitigation of the torsional response of the main structure, although it is likely to reduce the amplitude of the translational motion as well.

Finally, for the third system, only one damper is considered. The damper is to be located such that its center of mass coincides with the center of rotation of the main structure.

For each considered system, numerical analyses are carried out by following the procedure given above to identify the optimum TMD system. For the analysis, the wind forces are simulated according to Eqs. (5) to (7) for the values of $\alpha = 1.5$, $\sigma_F = 27340$ and $e_\sigma = 0.033$. Further, the analysis is first carried out by considering viscous damping mechanisms for the dampers, and then repeated by considering the power law damping mechanism for the dampers. Also, the impact of the amount of damping of the dampers on the response ratios is assessed.

3.3 TMD-structure System with Dampers with Viscous Damping Mechanism

By carrying out the analysis for the three considered TMD-structure systems, the obtained mean of the response ratios (m_{RY}, $m_{R\dot{\theta}}$ and $m_{R\ddot{Y}}$) are shown in Figures 2 to 4 for values of the correlation coefficient between $F_Y(t)$ and $M(t)$, $\rho_{F_Y M}$, and of frequency ratio r_f.

The results shown in Figure 2 for the first TMD-structure system suggest that the mean response ratios are affected by $\rho_{F_Y M}$ and that maximum reduction of the peak responses (i.e., minimum value of mean response ratios) occurs at different r_f values. However, the selection of the optimum TMD system is not significantly affected by the $\rho_{F_Y M}$ value.

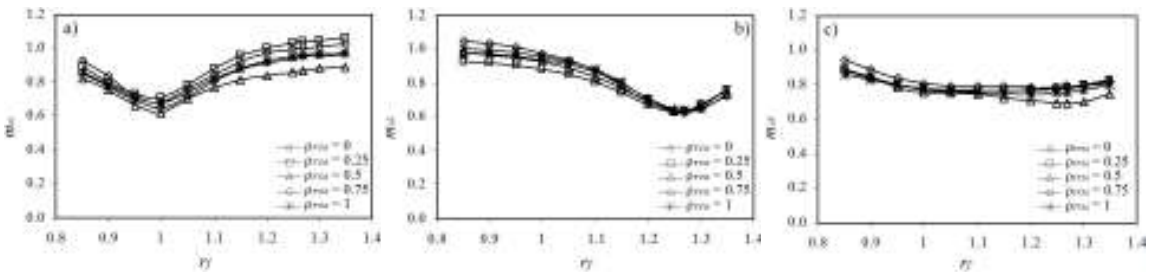

Figure 2: Expected value of the response ratios for the first TMD system as a function of the frequency ratio for TMDs with viscous damping: a) m_{RY}; b) $m_{R\dot{\theta}}$ and c) $m_{R\ddot{Y}}$.

In particular, Figure 2a shows that m_{RY} is significantly reduced for rf close to 1 and that for certain range of r_f and some values of $\rho_{F_Y M}$, m_{RY} exceeds 1, indicating that the use of dampers increases the response of the main structure. Figure 2b shows that the reduction in the peak rotational response can be achieved for r_f approximately equal to 1.27 (i.e., ω_θ/ω_Y). In other words, the dampers are tuned to the torsional frequency of the structure. However, the effectiveness of the dampers in reducing the acceleration response $\ddot{Y}_{prO}$ (Figure 2c) is somewhat insensitive to the value of r_f. This can be explained by noting that $\ddot{Y}_{prO}$ depends on both the translational and rotational accelerations. In all cases, the use of the TMD system effectively reduces the peak responses of the main structure.

Similar conclusions as above could be drawn based on the results shown in Figure 3 for the second TMD-structure system, and the reduction in responses for both TMD systems are similar as well. Therefore, use of two or three TMDs in reducing the peak responses for the considered structure is likely to be governed by the feasibility of the construction and installation of the TMDs.

The results for the third considered TMD-structure system are shown in Figure 4, it can be observed that the reduction in the peak translational displacement and $\ddot{Y}_{prO}$ is achieved for r_f close to 1. Note that for this case, since there is no reduction of the torsional responses, $m_{R\dot{\theta}}$ equals one for all values of r_f and is not shown.

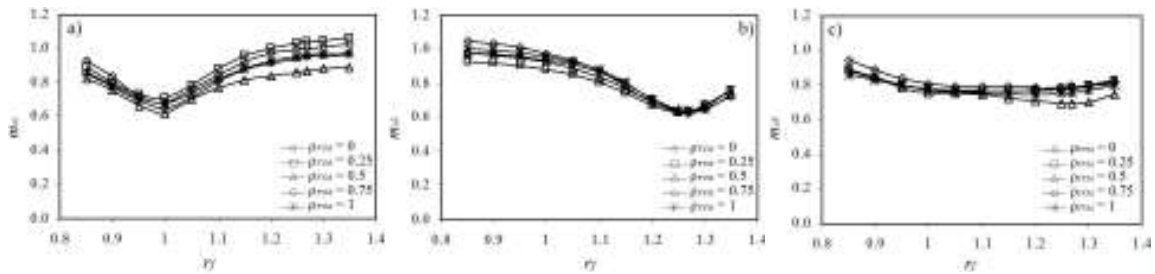

Figure 3: Expected value of the response ratios for the second TMD system as a function of the frequency ratio for TMDs with viscous damping: a) m_{RY} ; b) $m_{R\dot{\theta}}$ and c) $m_{R\ddot{Y}}$.

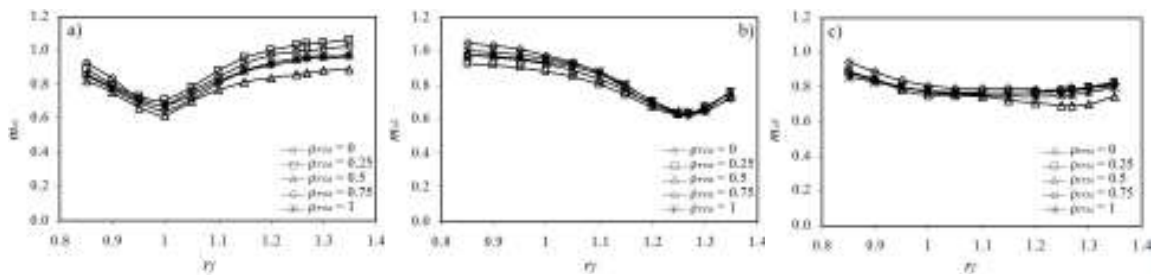

Figure 4: Expected value of the response ratios for the third TMD system as a function of the frequency ratio for TMDs with viscous damping: a) m_{RY} and b) $m_{R\ddot{Y}}$.

3.4 TMD-structure System with Dampers with Power Law Damping Mechanism

As mentioned earlier, the analysis carried out for TMD-structure systems with dampers with viscous damping mechanism is repeated but considering the power law damping mechanism for the dampers. The obtained results are shown in Figures 5 to 7. Comparison of the results shown in these figures to those presented in Figures 2 to 4 indicates that the conclusions drawn from the latter are equally applicable to the former.

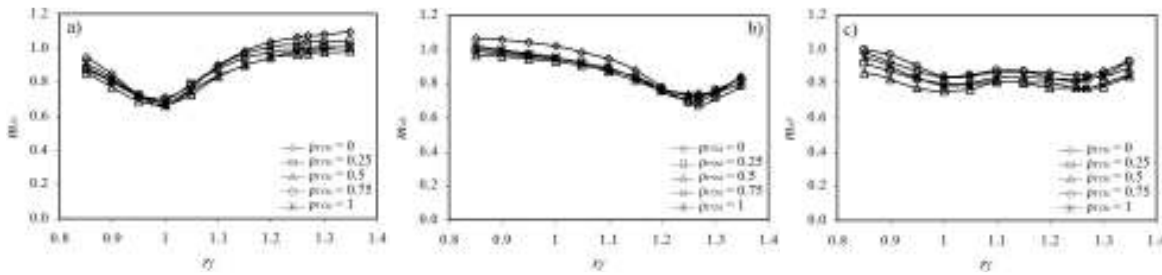

Figure 5: Expected value of the response ratios for the first TMD system as a function of the frequency ratio for TMDs with power law damping: a) m_{RY}; b) $m_{R\dot{\theta}}$ and c) $m_{R\ddot{Y}}$.

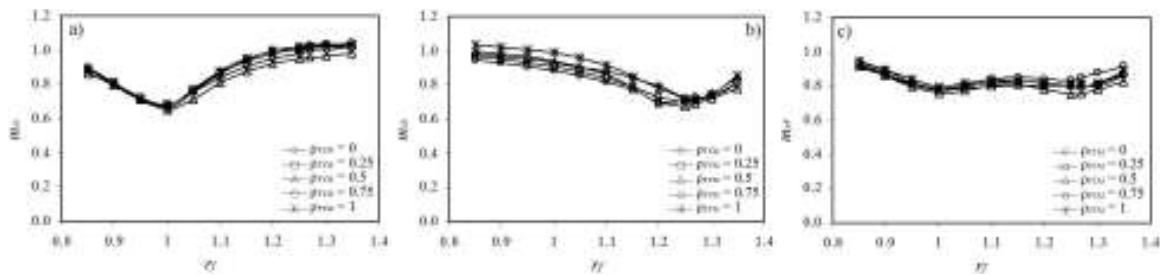

Figure 6: Expected value of the response ratios for the second TMD system as a function of the frequency ratio for TMDs with power law damping: a) m_{RY}; b) $m_{R\dot{\theta}}$ and c) $m_{R\ddot{Y}}$.

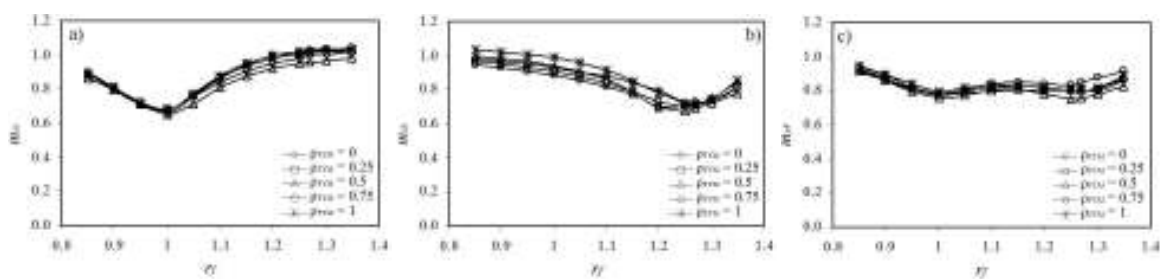

Figure 7: Expected value of the response ratios for the third TMD system as a function of the frequency ratio for TMDs with power law damping: a) m_{RY} and b) $m_{R\ddot{Y}}$.

Although is not the objective of the present study, a comparison of the effectiveness of the TMD-structure system with viscous and power law damping mechanisms indicates that the use of either one or the other is effective to reduce the structural response.

3.5 Effect of the Damping Coefficient of the Damper

The results presented in Figures 2 to 7 are obtained by considering the optimum damping coefficient of the damper(s). To illustrate the effect of the damping coefficient on the effectiveness of the TMDs in mitigating the structural response, an analysis is carried out in this section considering the

above mentioned three TMD-structure systems but varying the damper's damping coefficient. For the analysis, the frequency ratio r_f is selected equal to those identified optimum frequency ratios r_{fopt} based on the results presented in Figures 2 to 7.

The results from the analyses for the systems shown in Figure 2 to 7 are presented in Figures 8 to 13, respectively. The results show that the mean response ratios (m_{RY} , $m_{R\dot{\theta}}$ and $m_{R\ddot{Y}}$) vary with the ratio C_L/C_s or C_{PL}/C_s, and depend on the considered damping mechanism. In general for the dampers with the power law damping mechanism, the mean response ratio decreases as C_{PL}/C_s, increases. However, for the dampers with viscous damping mechanisms, the mean response ratio decreases initially as C_L/C_s increases, and a slight increase in the mean response ratio can be observed as C_L/C_s increases further (i.e., right side of the figures). This implies that a significant further increase in C_L/C_s is not effective in reducing the peak responses.

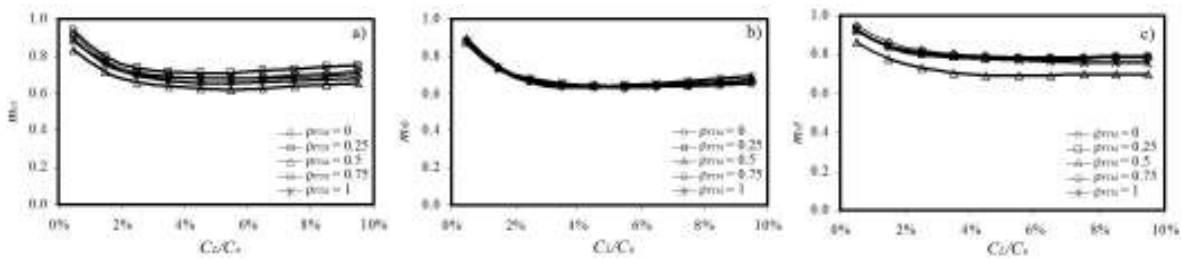

Figure 8: Expected value of the response ratios for the first TMD system as a function of the ratio CL/Cs for TMDs with viscous damping: a) m_{RY} ; b) $m_{R\dot{\theta}}$ and c) $m_{R\ddot{Y}}$.

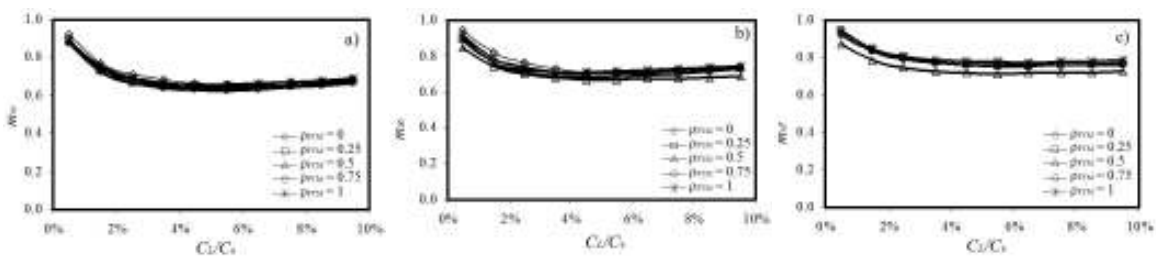

Figure 9: Expected value of the response ratios for the second TMD system as a function of the ratio CL/Cs for TMDs with viscous damping: a) m_{RY} ; b) $m_{R\dot{\theta}}$ and c) $m_{R\ddot{Y}}$.

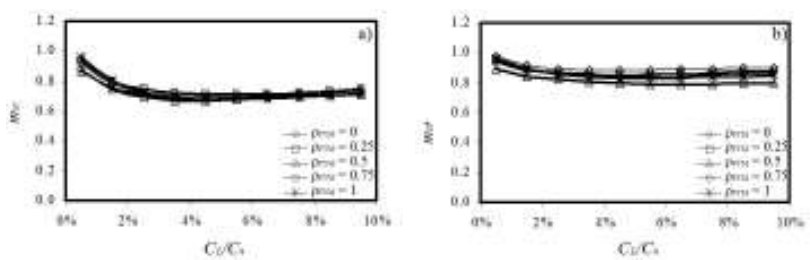

Figure 10: Expected value of the response ratios for the third TMD system as a function of the ratio CL/Cs for TMDs with viscous damping: a) m_{RY} and b) $m_{R\ddot{Y}}$.

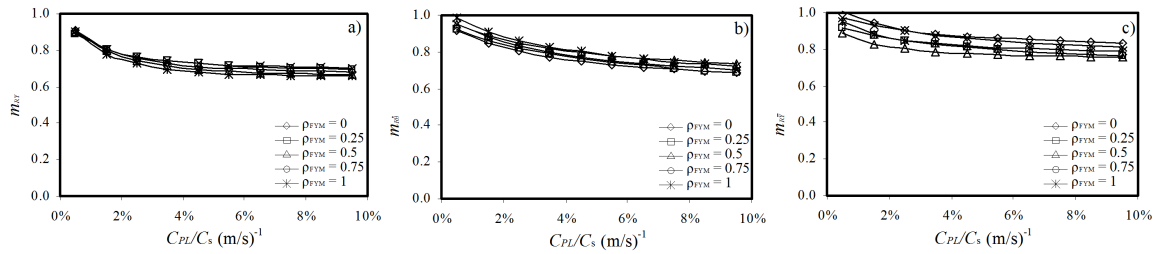

Figure 11: Expected value of the response ratios for the first TMD system as a function of the ratio CL/Cs for TMDs with power law damping: a) m_{RY} ; b) $m_{R\dot{\theta}}$ and c) $m_{R\ddot{Y}}$.

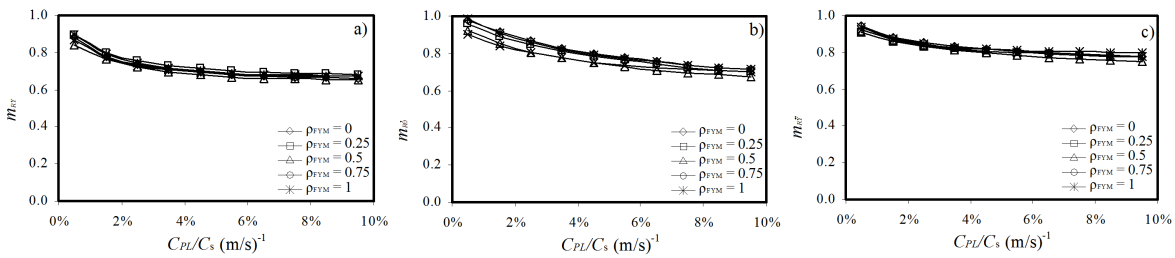

Figure 12: Expected value of the response ratios for for the second TMD system as a function of the ratio CL/Cs for TMDs with power law damping: a) m_{RY} ; b) $m_{R\dot{\theta}}$ and c) $m_{R\ddot{Y}}$.

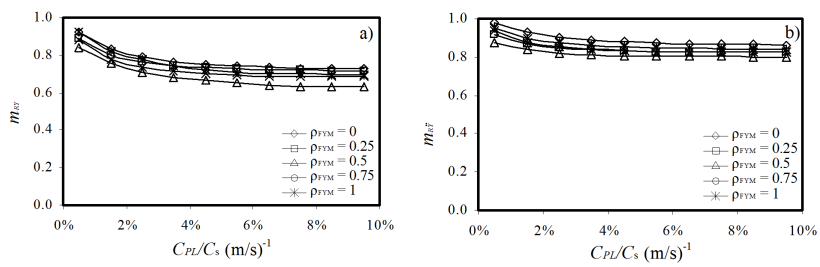

Figure 13: Expected value of the response ratios for the third TMD system as a function of the ratio CL/Cs for TMDs with power law damping: a) m_{RY} and b) $m_{R\ddot{Y}}$.

It is interest to note that at r_{fopt}, the dampers are effective for a considerable range of C_L or C_{PL} values.

3.6 Identified Optimum TMD System

The optimum parameters of the TMD systems for the considered structure are shown in Table 2. The results suggest that r_{fopt} can be considered to be independent of ρ_{F_YM} for the dampers with viscous damping mechanism and that the maximum reduction of the structural response is achieved when the dampers are tuned to the vibration frequency of the mode whose response is to be reduced. Table 2 also shows the results of the optimum parameters of TMD systems with power law

damping mechanism. Similar to the case with viscous damping, r_{fopt} for the dampers with power law damping mechanism could be considered to be independent of $\rho_{F_Y M}$.

Further parametric study considering different dynamic characteristics of the main structure as shown in Table 2 was also carried out and the identified optimum TMD systems for the TMDs with viscous and power law damping mechanism are summarized in Table 3. It shows that, in general, the optimum tuning frequency of the dampers is equal to the vibration frequency of the mode of the structure whose response is to be reduced (i.e., $r_{fopt} = 1$). This is the case for TMDs with viscous or power law damping mechanism. It is noted that values of r_{fopt} equal to ω_θ/ω_Y indicate that the frequency of the TMDs is to be tuned to the frequency of the torsional mode of the structure (i.e., ω_θ). Table 3 also shows that in most of the cases, the ratio C_{Lopt}/C_s is smaller than C_{PLopt}/C_s, this is because the TMDs with power law damping mechanism help the structure to attain the maximum reduction at higher values of C_{PL} as indicated previously. Moreover, inspection of Table 3 indicates that the ratios C_{Lopt}/C_s and C_{PLopt}/C_s are more dependent on the type of response considered than r_{fopt}.

Response	ρ_{FYM}	Linear damping mechanism						Power law damping mechanism					
		System 1		System 2		System 3		System 1		System 2		System 3	
		r_{fopt}	C_{Lopt}/C_s	r_{fopt}	C_{Lopt}/C_s	r_{fopt}	C_{Lopt}/C_s	r_{fopt}	C_{PLopt}/C_s	r_{fopt}	C_{PLopt}/C_s	r_{fopt}	C_{PLopt}/C_s
m_{RY}	0	1	0.055	1	0.055	1	0.055	1	0.095	1	0.095	1	0.095
	0.25	1	0.045	1	0.045	1	0.055	1	0.095	1	0.095	1	0.095
	0.5	1	0.055	1	0.045	1	0.065	1	0.095	1	0.095	1	0.095
	0.75	1	0.045	1	0.045	1	0.045	1	0.095	1	0.095	1	0.095
	1	1	0.045	1	0.035	1	0.045	1	0.095	1	0.095	1	0.095
$m_{R\dot{\theta}}$	0	1.27	0.070	1.27	0.070	-	-	1.25	0.119	1.27	0.121	-	-
	0.25	1.27	0.070	1.27	0.057	-	-	1.25	0.119	1.25	0.119	-	-
	0.5	1.27	0.070	1.27	0.057	-	-	1.25	0.119	1.25	0.119	-	-
	0.75	1.27	0.057	1.27	0.070	-	-	1.25	0.119	1.2	0.114	-	-
	1	1.27	0.057	1.27	0.057	-	-	1.27	0.121	1.27	0.121	-	-
$m_{R\ddot{Y}}$	0	1.27	0.083	1.27	0.070	1	0.045	1	0.095	1	0.095	1	0.095
	0.25	1.27	0.070	1.27	0.083	1	0.045	1.25	0.119	1	0.095	1	0.095
	0.5	1.27	0.070	1.27	0.070	1	0.065	1	0.095	1.25	0.119	1	0.095
	0.75	1.27	0.083	1.27	0.083	1	0.045	1.25	0.119	1	0.095	1	0.095
	1	1.27	0.121	1.27	0.083	1	0.055	1	0.095	1	0.095	1	0.095

Table 2: Optimum values of the TMD system for the structure considered.

Structure			Linear damping mechanism						Power law damping mechanism					
			System 1		System 2		System 3		System 1		System 2		System 3	
No.	ω_s (rad/s)	ω_θ/ω_s	r_{fopt}	C_{Lopt}/C_s	r_{fopt}	C_{Lopt}/C_s	r_{fopt}	C_{Lopt}/C_s	r_{fopt}	C_{PLopt}/C_s $(m/s)^{-1}$	r_{fopt}	C_{PLopt}/C_s $(m/s)^{-1}$	r_{fopt}	C_{PLopt}/C_s $(m/s)^{-1}$
1	0.787	0.25	1	0.05	1	0.04	1	0.04	1	0.11	1	0.12	1	0.03
2	0.787	0.5	1	0.05	1	0.05	1	0.03	0.98	0.11	1	0.14	1	0.03
3	0.787	0.75	1	0.05	1	0.05	1	0.03	1	0.09	1	0.14	1	0.03
4	0.787	1	1	0.05	1	0.04	1	0.02	1	0.11	1	0.13	1	0.03
5	0.787	1.27	1	0.05	1	0.04	1	0.02	1	0.11	1	0.14	1	0.04
6	0.787	1.5	1	0.05	1	0.06	1	0.03	1	0.13	1	0.09	1	0.03
7	0.787	1.75	1	0.04	1	0.05	1	0.03	1	0.14	1	0.12	1	0.03
8	0.787	2	1	0.04	1	0.06	1	0.02	1	0.14	1	0.11	1	0.03
9	1	0.25	1	0.04	1	0.05	1	0.03	1	0.15	1	0.15	1	0.06
10	1	0.5	1	0.05	1	0.05	1	0.03	1	0.15	0.5	0.05	1	0.08
11	1	0.75	1	0.05	1	0.05	1	0.03	1	0.15	1	0.15	1	0.05
12	1	1	1	0.06	1	0.06	1	0.03	1	0.15	1	0.15	1	0.05
13	1	1.25	1	0.06	0.95	0.05	1	0.03	1	0.15	1	0.15	1	0.05
14	1	1.5	1	0.04	1	0.05	1	0.03	1	0.15	1	0.15	1	0.04
15	1	1.75	1	0.05	1	0.05	1	0.03	1	0.15	1	0.15	1	0.040
16	1	2	1	0.05	1	0.04	1	0.03	1	0.15	1	0.15	1	0.040

Table 3a: Optimum values of the TMD system to reduce m_{RY} considering different damping mechanisms and configurations.

Structure			Linear damping mechanism				Power law damping mechanism			
			System 1		System 2		System 1		System 2	
No.	ω_s (rad/s)	ω_θ/ω_s	r_{fopt}	C_{Lopt}/C_s	r_{fopt}	C_{Lopt}/C_s	r_{fopt}	C_{PLopt}/C_s $(m/s)^{-1}$	r_{fopt}	C_{PLopt}/C_s $(m/s)^{-1}$
1	0.787	0.25	0.25	0.013	0.25	0.01	0.25	0.038	0.25	0.038
2	0.787	0.5	0.5	0.025	0.5	0.035	0.5	0.075	0.5	0.075
3	0.787	0.75	0.75	0.03	0.75	0.045	0.75	0.113	0.75	0.113
4	0.787	1	1	0.05	1	0.06	1	0.05	1	0.050
5	0.787	1.27	1.25	0.063	1.25	0.088	1.25	0.188	1.27	0.191
6	0.787	1.5	1.5	0.075	1.45	0.102	1.45	0.218	1.5	0.225
7	0.787	1.75	1.725	0.086	1.725	0.104	1.725	0.259	1.725	0.259
8	0.787	2	1.95	0.098	1.95	0.098	2.01	0.302	1.95	0.293
9	1	0.25	0.75	0.008	0.7	0.007	0.7	0.007	0.7	0.007
10	1	0.5	0.5	0.025	0.5	0.03	0.5	0.075	1.05	0.158
11	1	0.75	0.75	0.04	0.75	0.038	0.75	0.113	0.75	0.113
12	1	1	1	0.06	1	0.06	1	0.06	1	0.100
13	1	1.25	1.25	0.063	1.25	0.075	1.2	0.18	1.2	0.180
14	1	1.5	1.5	0.09	1.5	0.09	1.5	0.225	1.5	0.225
15	1	1.75	1.75	0.105	1.725	0.121	1.725	0.259	1.725	0.259
16	1	2	1.975	0.099	1.98	0.06	1.95	0.293	1.9	0.285

Table 3b: Optimum values of the TMD system to reduce $m_{R\dot{\theta}}$ considering different damping mechanisms and configurations.

Structure			Linear damping mechanism						Power law damping mechanism					
			System 1		System 2		System 3		System 1		System 2		System 3	
No.	ω_s (rad/s)	ω_θ/ω_s	r_{fopt}	C_{Lopt}/C_s	r_{fopt}	C_{Lopt}/C_s	r_{fopt}	C_{Lopt}/C_s	r_{fopt}	C_{PLopt}/C_s $(m/s)^{-1}$	r_{fopt}	C_{PLopt}/C_s $(m/s)^{-1}$	r_{fopt}	C_{PLopt}/C_s $(m/s)^{-1}$
1	0.787	0.25	1	0.05	1	0.04	1	0.04	1	0.15	1	0.12	1	0.03
2	0.787	0.5	0.5	0.02	0.5	0.03	1	0.03	0.5	0.075	0.5	0.075	1	0.02
3	0.787	0.75	0.75	0.045	0.75	0.06	1	0.03	0.75	0.113	0.75	0.113	1	0.02
4	0.787	1	1	0.05	1	0.06	1	0.01	1	0.14	1	0.11	1	0.01
5	0.787	1.27	1	0.08	1.2	0.12	1	0.02	1.25	0.188	1.2	0.18	1	0.02
6	0.787	1.5	1	0.06	1.05	0.158	1	0.03	1.5	0.225	1	0.15	1	0.04
7	0.787	1.75	1	0.04	1	0.06	1	0.03	1	0.15	1	0.12	1	0.04
8	0.787	2	1	0.07	1	0.07	1	0.02	1	0.15	1	0.15	1	0.02
9	1	0.25	1	0.05	1	0.06	1	0.03	1	0.15	1	0.15	1	0.04
10	1	0.5	0.5	0.025	0.5	0.025	1	0.02	0.5	0.075	0.5	0.075	1	0.04
11	1	0.75	0.75	0.038	0.75	0.053	1	0.02	0.75	0.113	0.775	0.116	1	0.03
12	1	1	1	0.05	1	0.06	1	0.01	1	0.10	1	0.12	1	0.01
13	1	1.25	1.25	0.088	1.25	0.10	1	0.02	1	0.15	1.05	0.158	1	0.05
14	1	1.5	1.5	0.09	1	0.08	1	0.03	1	0.15	1	0.15	1	0.03
15	1	1.75	1	0.05	1	0.06	1	0.03	1	0.15	1	0.15	1	0.050
16	1	2	1	0.05	1	0.06	1	0.03	1	0.15	1	0.15	1	0.030

Table 3c: Optimum values of the TMD system to reduce $m_{R\ddot{Y}}$ considering different damping mechanisms and configurations.

4 CONCLUSIONS

The analysis of structures with TMDs to reduce the wind induced peak response is carried out. For the analysis the wind loading is simulated based on commonly used power spectral density of wind load. The analysis results show that the peak responses can be reduced with the use of TMDs with linear and nonlinear damping mechanisms. More specifically, it is concluded that:

1) The mean response ratios are affected by the correlation coefficient between the total horizontal force and the torsional moment; however, the selection of the optimum TMD system is not significantly affected by it.
2) The use of two or three TMDs in reducing the peak responses (in particular the torsional response) for the considered structures is likely to be governed by the feasibility of the construction and installation of the TMDs.
3) In general, for the dampers with the power law damping mechanism, the mean response ratio decreases as the ratio between the damping coefficient whit power law mechanism to the damping coefficient of the main structure increases.
4) The use of TMDs with viscous damping mechanism is not effective for large values of the coefficient of viscous damping.

5) In general the optimum tuning frequency of the dampers is equal to the vibration frequency of the mode of the structure whose response is to be reduced.
6) The ratios of the optimum coefficient of viscous damping to the coefficient of damping of the main structure and the optimum coefficient of power law damping to the coefficient of damping of the main structure are more dependent on the type of response considered compare to the optimum frequency ratio.

Acknowledgements

The financial supports of the National Council for Science and Technology (CONACYT) of Mexico, and the University of Western Ontario are gratefully acknowledged. We thank Jon K. Galsworthy for many fruitful discussions, constructive comments and suggestions during the development of this work.

References

Bakre SV, Jangig RS. 2007. Optimum parameters of tuned mass damper for damped main system. Structural Control and Health Monitoring, 14: 448 – 470.

Chen PW, Robertson LE. 1972. Human perception thresholds of horizontal motion. Journal of the Structural Division, ASCE, 98: 1681-1695.

Den Hartog JP. 1956. Mechanical Vibrations, McGraw-Hill, New York.

Di Paola M. 1998. Digital simulation of wind field velocity. Journal of Wind Engineering and Industrial Aerodynamics, 74-76: 91-109.

Fujino Y, Abe M. 1993.Design formulas for tuned mass dampers based on a perturbation technique. Earthquake Engineering and Structural Dynamics, 22: 833-854.

Haupt LR, Haupt SE. 2004. Practical genetic algorithms. Hoboken, N.J.: Wiley-Interscience.

Housner GW, Bergman LA, Caughey TK, Chassiakos AG, Claus RO et al. 1997. Structural control: Past, present and future. Journal of Engineering Mechanics, ASCE, 123: 897-971.

Irwin AW. 1978. Human response to dynamic motion of structures. The Structural Engineer, 56A(9): 237-244.

Isyumov N. 1993. Criteria for acceptable wind-induced motions of tall buildings. International Conference on Tall Buildings, Council on Tall Buildings and Urban Habitat, Rio de Janeiro.

Isyumov N. Motion perception, tolerance and mitigation. 1995. 5th World Congress of the Council of Tall Buildings and Urban Habitat, Amsterdam, The Netherlands.

Jangid RS, Datta TK. 1997. Performance of multiple tuned mass dampers for torsionally coupled system. Earthquake Engineering and Structural Dynamics, 26: 307-317.

Li C, Qu W. 2006. Optimum properties of multiple tuned mass dampers for reduction of translational and torsional response of structures subjected to ground acceleration. Engineering Structures, 28: 472-494.

Mattei M and Ricciardelli F. 2002. Mathematical model for design of mass dampers for wind excited structures. Journal of Engineering Mechanics, 128: 9, 979-988.

Melbourne WH, Palmer TR. 1992. Accelerations and comfort criteria for buildings undergoing complex motions. Journal of Wind Engineering and Industrial Aerodynamics, 41-44: 105-1116.

Mendis P, Ngo T, Haritos N, Hira A, Salami B, Cheung J. 2007. Wind loading on tall buildings, Electronic Journal of Structural Engineering , Special issue: 41-54.

Pansare AP, Jangid RS. 2003. Tuned mass dampers for torsionally coupled systems, Wind and Structures, 6(1): 23-40.

Pozos-Estrada, A., Hong, H.P., Galsworthy, J.K. 2010. Serviceability design factors for wind-sensitive structures. Can. J. Civ. Eng., 37: 728-738.

Pozos-Estrada, A., Hong H.P., and Galsworthy, J.K. 2011. Reliability of Structures with Tuned Mass Dampers under Wind-induced Motion: A Serviceability Consideration. Wind and Structures an International Journal, Vol. 14(2), pp. 1 – 19.

Rüdinger F. 2007a. Tuned mass damper with nonlinear viscous damping. Journal of Sound and Vibration, 300: 932–948.

Rüdinger F. 2007b. Response Spectral Density for Oscillators with Nonlinear Damping Journal of Engineering Mechanics, 133(3): 278-289.

Ricciardelli F, Vickery BJ. 1999. Tuned vibration absorber with dry friction damping, Earthquake Engineering and Structural Dynamics, 28: 707-723.

Shinozuka M. 1972. Monte Carlo solution of structural dynamics. Technical report No. 19, Columbia University, New York.

Simiu E, Scanlan RH. Wind Effects on Structures: Fundamentals and Applications to Design, Wiley, New York, 1996.

Soong TT and Costantinou MC. 1994. Passive and active structural vibration control in civil engineering. Springer-Verlag, Wien.

Terenzi, G. 1999. Dynamics of SDOF systems with nonlinear viscous damping. Journal of Engineering Mechanics, 125: 956-963.

Tsai HC, Lin GC. 1983. Explicit formulae for optimum absorber parameters for forced excited and viscously damped systems. Journal of Sound and Vibration, 89: 385–396.

Vanderplaats GN. 1984. Numerical optimization techniques for engineering design: with applications, New York ; Montreal : McGraw-Hill.

Vickery BJ, Galsworthy JK, Gerges R. 2001. The behaviour of simple non-linear tuned mass dampers. 6th World Congress of the Council on Tall Buildings and Urban Habitat, Melbourne, Australia.

Wang J-F, Lin C-C, Lian C-H. 2009. Two-stage optimum design of tuned mass dampers with consideration of stroke. Structural Control and Health Monitoring, 14: 448 – 470.

Warburtun G, Ayorinde E. 1980. Optimum absorber parameters for simple systems. Earthquake Engineering and Structural Dynamics, 8: 197-217.

Warburtun G. 1982. Optimum absorber parameters for various combinations of response and excitation parameters. Earthquake Engineering and Structural Dynamics, 10: 381- 401.